# Soft Matter

Accepted Manuscript






ROYAL SOCIETY OF CHEMISTRY

www.rsc.org/softmatter

Journal Name

RSCPublishing

ARTICLE

# Mechanical and Structural Comparison between Primary Tumor and Lymph Node Metastases Cells in Colorectal Cancer

Cite this: DOI: 10.1039/x0xx00000x

Received 00th January 2012,
Accepted 00th January 2012

DOI: 10.1039/x0xx00000x

www.rsc.org/

V. Palmieri [a*], D. Lucchetti [b*], A. Maiorana [a], M. Papi [a#], G. Maulucci [a], Federica Calapà [b], G. Ciasca [a], R. Giordano [a], A. Sgambato [b&] and M. De Spirito [a&]

**Abstract** The SW480 and SW620 colon carcinoma cell lines derive from the primary tumour and a lymph-node metastasis of the same patient, respectively. For this reason, these cells represent an ideal system to analyse phenotypic variations associated with the metastatic process. In this study we analysed the SW480 and SW620 cytoskeleton remodelling by measuring the cells mechanics and morphological properties using different microscopic techniques. We observed that the different specialized functions of cells, i.e. the capacity to metastasize of elongated cells inside the primary tumour and the ability to intravasate and resist to shear forces of the stream of cells derived from the lymph node metastasis, are reflected in their mechanical properties. We demonstrated that, together with the stiffness and the adhesion between the AFM tip and cell surface, cell shape, actin organization and surface roughness are strictly related and are finely modulated by the colorectal cancer cells to better accomplish their specific tasks in cancer growth and invasion.

## Introduction

Cancer mechanics is the study of forces involved in the intricate interplay between cells and extracellular environment. The emerging idea in this research field is that forces acting on cells can control biochemical signals responsible for cell proliferation, migration and apoptosis[1]. Cells sense and respond to the mechanical properties of the environment, such as the stiffness of the extracellular matrix (ECM) or the compression exerted by neighbouring tissues, by balancing external forces with changes in cytoskeleton and shape remodelling[2, 3]. This response leads to the activation of signalling pathways of cells spreading, growth, motility and death[4].

The study of the forces that link environment and tumour cells can help to understand the metastatic process, leading cause of mortality among cancer patients. During this process, cells of the primary tumour detach from neighbours, remodel the external matrix and migrate towards the vasculature and lymphatics. These processes require dynamic modulation of cell shape and cytoskeleton together with changes in gene expression[4]. For example, metastatic cells can detach by altering surface proteins expression and reducing adhesion or by altering cytoskeleton polymerization in order to acquire a higher plasticity, increase the number of protrusions and squeeze easily through ECM[1].

Specific cellular and extra-cellular mechanical properties have been exploited as possible biomarkers of cancer progression in the hope of identifying physical attributes that would allow recognizing cells that are more likely to metastasize[5, 6].

In this study, we compared the mechanical and morphological features of colon cancer cell populations isolated from a tumour and from lymphatic metastases of the same tumour[6-8].

Colon cancer develops in the bowel, grows through the muscle layer of the colon or rectum and subsequently can spread to lymph nodes in the area close to the bowel. The dissemination of cancer cells in local lymph nodes represents an important prognostic factor[9].

To study the mechanical and morphological changes that lead to the acquisition of metastatic ability, we used the SW480 and SW620 cell lines that offer unique advantages for the colon cancer study representing two different steps of cancer disease.

SW480 and SW620 cells were isolated from a primary colon cancer in the early phase and from a lymph node metastasis developed months later by the same patient, respectively[7].

For their limited genetic variability, these cells are considered a suitable and validated model of colon cancer progression and are frequently used to investigate genetic and proteic changes associated with different phases of colon cancer development[7, 10].

We analysed a set of cell parameters. First, the cell shape, membrane protrusions and surface Roughness have been studied by means of Scanning Electron Microscopy (SEM). The SW480 cell line showed an increased surface roughness and protrusion appearance in respect to the SW620 cells. Since the spatial reorganization of cytoskeleton structure directly affects cell shape and surface Roughness[11], we used Atomic Force Microscopy (AFM) and Confocal Microscopy to probe the cytoskeleton structure. Alterations in cytoarchitecture are known to increase Elasticity and/or cell deformability and are associated with malignant transformation[12]. By means of AFM, the Cell Stiffness was quantified in terms of Young Modulus. AFM was also used to quantify changes in non-specific cell Adhesion between the cantilever and cell surface during metastases. The physics of adhesion between biological cells significantly influences and is modulated during cancer cell movement, invasion and metastasis. Indeed tumor cells must exhibit considerable flexibility in their adhesive interactions since a distant metastatic formation is strongly influenced by the new stable adhesions between cancer cells and the vessel walls[13]. Both specific and non-specific forces together contribute to cell adhesion and spreading processes [14, 15]. Non specific forces between the cell membrane and the surrounding tissues, based on van der Waals attraction and hydrophobic/hydrophilic interplay, are continually modulated during the cancer cells migration to fit the cancer cells environment. Recent papers have reported that while specific Adhesions of malignant cancer cells are often reduced to facilitate their detachment from the parent tumour, the high non-specific Adhesion force on them can strategically maximize their adherence and invasion to diverse tissues during metastasis[16]. We also observed an increase in Adhesion between the cantilever and surface of metastatic cells which can result in a better cell attachment to the vessel walls.

Finally, the variations in cell mechanics, probed with AFM, were directly related to the structure of actin network imaged with Confocal Microscopy. We found that cells during different stages of tumour progression modulate the cytoskeleton architecture to detach from the primary tumour or acquire new growth capacities or the ability to use "voluntarily" non-specific interactions to become "sticky" in the lymph node. Overall, in this paper we measured several parameters differently related to the cell architecture to shed light on biomechanical regulation of tumour progression.

## Results and discussion

It has been previously reported[8, 15] that SW480 and SW620 cells have different appearance in culture: most SW480 cells have a spreading, epithelial-type morphology (E-type), while a small fraction displays a rounded morphology (R-type). The existence of two distinct and independent subpopulations, displaying different growth and tumorigenic abilities within the SW480 cell line has been previously demonstrated and it was shown that they stably maintain their morphologies in colture. Cell cycle analysis performed by us (data not shown) as well by other groups hasn't evidenced differences in cell cycle distribution between the two subpopulations[8].

In contrast, SW620 cells are known to display an ovoid morphology and form small aggregates[8].

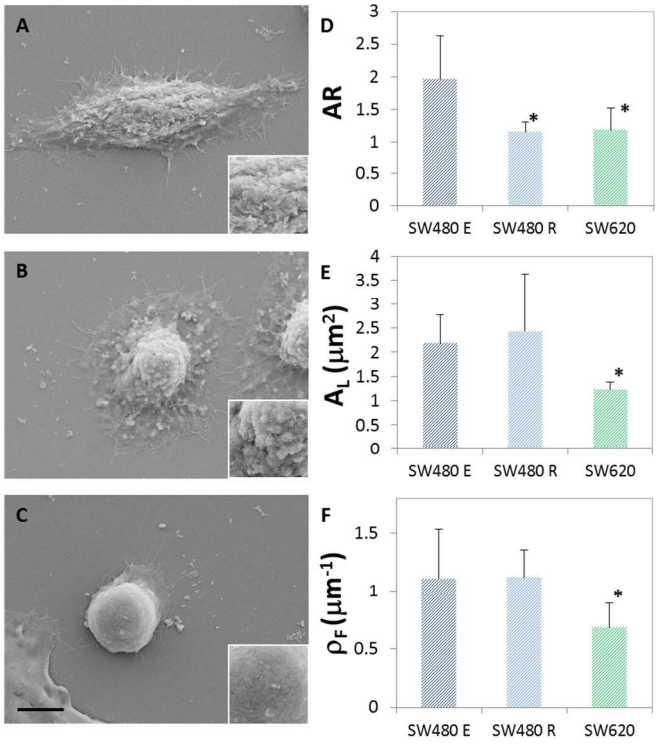


**Fig. 1 SEM Morphological characterization of SW480 (E-type or R type) and SW620 cells.** SW480 cells comprise an elongated (E-type) (A) and a rounded (R-type) (B) population both showing a large lamellipodia area with fine protrusions emanating from it. On the contrary, SW620 cells have a rounded morphology with a reduced number of protrusions and a less extended lamellipodia area (C). In the insets a particular of cell surface is shown to evidence the different roughness. Scale bar is 10 μm. (D) The SW480 line can be divided in two distinct populations using a threshold based on Aspect Ratio of the cells. Indeed elongated cells (E-type) have a mean AR around 2 while rounded cells (R-type) have AR of 1. The SW620 cells displayed always aspect ratio always minor than 1.5 so they were not divided in sub-populations. Both E-type and R-type cells display a larger lamellipodia area (E) and a higher density of filopodia (F) compared to SW620 cells. Error bars in the graphs represent SD. Statistically significant results are marked by an asterisk ($p<0.001$ one-way ANOVA and Tukey's multiple comparison tests).

We observed clear morphological differences in SEM micrographs (Fig.1 and Fig.1S) with a prevailing rounded shape for SW620 cells (Fig. 1C) and mixed elongated (~ 90%) and rounded morphology in the SW480 cultures (Fig. 1 A and B). E-type and R-type cells in the SW480 line were analysed separately as previously described[17]: cells having an Aspect Ratio (AR, the ratio between minor and major axis of the cell) higher than 1.5 were considered E-type cells (Fig. 1D).

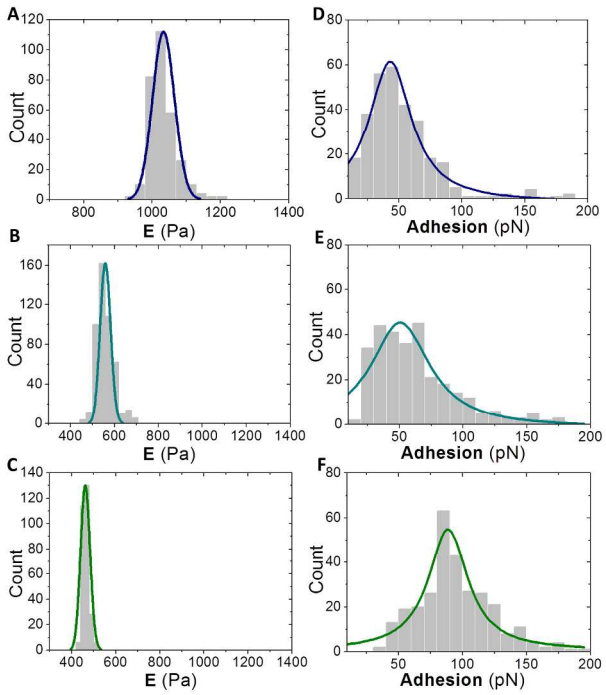


**Fig.2 Young Moduli of SW480 cells (E-type in A and R-type in B) compared to SW620 cells (C).** Cells with the highest Young modulus were SW480 E-type, which exhibited a larger distribution peaked at 1060 Pa. Both R-type SW480 and SW620 cells exhibited a narrower distribution peaked at 580 Pa and 480 Pa respectively, hence displaying a ''softer'' cytoskeleton. **Non-specific cell Adhesion of SW620 cells (F)** was significatively higher than in E-type **(D)** and R-type **(E)** SW480 cells.

In SW620 cells the AR never exceeded 1.5 (Fig. 1D). This criterion based on AR has been used also for measurements performed with AFM and Confocal Microscopy.

The membrane protrusions of SW480 and SW620 cells appeared markedly different in SEM micrographs. In Fig.1 A and B a large area around the cell body of SW480 cells is visible with thin filaments protruding from it. These structures are respectively the lamellipodia and filopodia, highly dynamic thin cell wall extensions of actin filaments. SW620 cells displayed a less extended lamellipodia area (Fig. 1C).

Differences observed in membrane protrusions were quantified by means of two parameters: density of filopodia along the cell perimeter ($\rho_F$) and Lamellipodia Area ($A_L$). The SW480 cells displayed a higher $\rho_F$ and a larger $A_L$ in respect to SW620 cells (Fig.1 E and F). It is important to note also a sharp difference in cell surface roughness in SEM micrographs. Indeed SW620 display a much smoother membrane compared to both populations of SW480 line (insets in Fig. 1 A, B and C). These surface differences can be a consequence of temporal and spatial reorganizations of cytoskeleton structure, which directly affects cell shape and surface roughness. Indeed the plasma membrane is directly attached to the actin filament by spectrin and ankyrins, a family of adaptor proteins that mediate the attachment of integral membrane proteins to the spectrin-actin based membrane cytoskeleton[11].

Cytoskeleton mechanical properties were analysed by means of Atomic Force Microscopy (AFM), recording stress-strain characteristics (force deformation curves) on cell surface (see Fig.5 for a representative AFM curve for each cell type). From the obtained curves, cell stiffness (Young Modulus) and non-specific Adhesion between the cantilever and cell surface were derived (see Experimental Section for details).

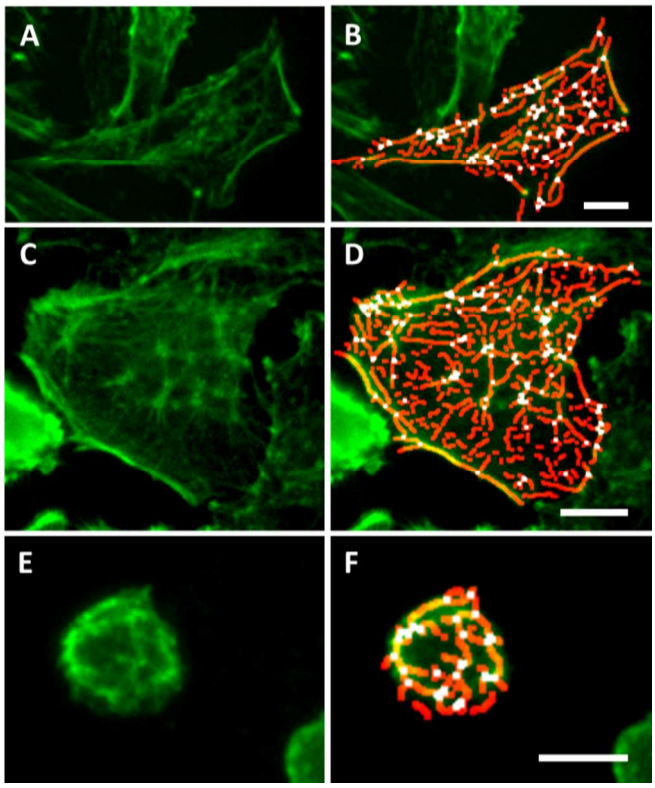


**Fig.3 Representative confocal images of skeletonized actin in SW480 E-type (A, B), SW480 R-type (C, D) and SW620 cells (E, F).** Skeleton branches are labelled in orange and junctions in white. For each cell the original image (A, C, E) and the actin skeleton (B, D, F) are shown. To enhance the contrast, the actin skeleton has been dilated in the superimposed images. Scale Bar are 10 μm.

Young Moduli of SW480 E-type or R-type and SW620 cells are shown in Fig.2 A, B, and C respectively. SW480 E-type cells displayed the highest values of Young modulus, with a wide distribution peaked at 1060 Pa. Both R-type SW480 and SW620 cells exhibited a narrower distribution peaked at 580 Pa and 480 Pa respectively, hence displaying a ''softer'' cytoskeleton. The low values of Young moduli measured (below 1 kPa) for all cell lines considered in this study, indicate a high deformability and compliance, typical of malignant phenotypes[13].

The non-specific Adhesion between the cantilever and cell surface distributions of SW480 E-type, SW480 R-type and SW620 cells are shown in Fig. 2D, E and F, respectively. The metastatic line SW620 displayed the highest Adhesion values with a distribution peaked at 95 pN. The two populations of SW480 cell line showed comparable Adhesion values with averages around 50 pN, in accordance to the similar surface roughness observed in SEM micrographs (insets in Fig. 1A and 1B) which is known to be strongly related to cell Adhesion properties at the nanoscale[18].

The high values of non-specific Adhesion between the cantilever and cell, the smooth surface topography and the decreased number of protrusions observed in the SW620 cells suggested an altered actin organization. Indeed recently, several experiments have linked variation of non-specific Adhesion with altered cytoskeleton organization using standard conditions and a treatment with toxic agents like cytochalasin D or colchicine, known to affect the polymerisation properties of actin and tubulin cytoskeletal components, respectively[19, 20].
We imaged actin network organization with Confocal Microscopy. In Fig. 2S representative confocal micrographs of SW480 and SW620 cells are shown with actin stained with Phalloidin in green and cell nuclei stained with Dapi in cyan.
In order to establish cytoskeleton organization differences among cell lines, two parameters were considered: actin fibers Coherency and Density of Junctions of actin network ($\rho_J$).
Coherency was calculated from the structure tensor of each pixel in the image and is bounded between 0 (isotropic areas) and 1 (highly oriented structures)[21]. Analysis of Coherency was performed on the original confocal images according to the procedure described in the Experimental section. In Fig. 3, representative confocal images with the skeletonized actin filaments of SW480 E-type (A, B), SW480 R-type (C, D) and SW620 cells (E, F) are shown. Analysis of skeletonized images allowed underlining actin branches (orange) and junctions (white).

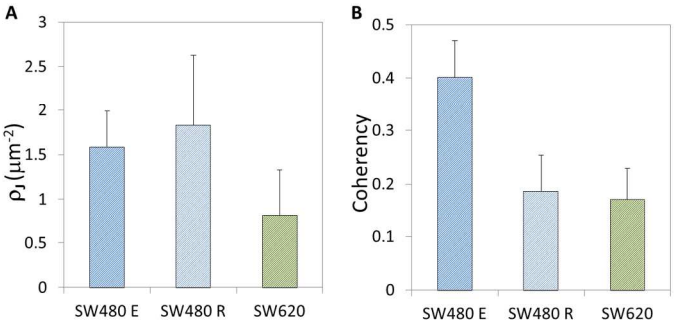


**Fig.4 Analysis of actin organization** (A) Average density of cytoskeleton junctions, normalized to cell area, obtained after skeletonization of actin network on confocal images. The number of junctions is highly reduced only in the SW620 cells. (B) Coherency of cytoskeleton obtained with OrientationJ plugin. Coherency is bounded between 0 and 1, with 1 indicating highly oriented structures and 0 indicating isotropic areas. Error bars represent SD. The coherency is markedly reduced in SW480-R and SW620 cells. Statistically significant results are marked by an asterisk ($p<0.001$ one-way ANOVA and Tukey's multiple comparison tests).

Image analysis revealed that, as expected from the lower stiffness values, the rounded cells have a decreased Coherency (Fig. 4b). Indeed we measured a mean value of Coherency of 0.4 for E-type SW480 cells and around 0.2 for R-type SW480 cells and SW620 cells. On the other hand, the increased Adhesion between the cantilever and cell surface together with the reduced number of junctions are markers of an actin network destructuration in SW620 cells (Fig. 4a).
To control their migratory and invasive capabilities, cancer cells are able to reorganize both their membrane protrusions and cytoskeleton[22, 23]. Filopodia and lamellipodia protrusions drive cell migration by attaching to the substrate and generating forces to pull the cell body forward, while cytoskeleton organization influences cell shape and mechanics as well as cell response to external forces[24]. Protrusions and, more importantly, cytoskeleton subversion in cancer cells can lead to changes in cell growth, stiffness, movement and invasiveness[25].
In order to analyse cytoskeleton of metastastic and non-metastatic cells, different high resolution techniques were used in this study. Filopodia and lamellipodia protrusions and cell surface morphology were analysed by SEM. Mechanical cell parameters (Elasticity and Non-specific cell Adhesion) were obtained recording Force-Distance Curves on cell surface by AFM. Actin cytoskeleton organization was quantified by measuring fibers anisotropy (Coherency) and networking (Junctions density) by image analysis of Confocal Microscopy measurements.
The specialized functions of SW480 populations, i.e. proliferate at the primary site (SW480 R-type) or metastasize (SW480 E-type), are reflected in cell shape and mechanical properties. We observed that SW480 R-type display a rounded morphology with a decreased Stiffness and actin Anisotropy (Coherency) compared to E-type cells.
The decrease of cell Stiffness can be a consequence of a destructuration of actin bundles (reduced Coherency) and therefore can represent a mechanistic pathway that drives uncontrolled growth and evasion of apoptosis[1]. Indeed, the actin cytoskeleton is a major determinant for normal tissue homeostasis. Firstly, actin interacts with adhesion molecules and regulates stability and dynamics of cell-cell junctions, which maintain tissue integrity and allow tissue remodelling. Secondly, actin determines cell polarity through the localization of specific proteins in cell membrane specific areas, enabling cells to carry out specialized functions. When cell polarity is lost, tissue integrity is compromised, resulting in overgrowth, aberrant invasive behaviour and promotion of tumours[25].
The higher cell deformability and actin isotropy in rounded cells are also markers of their well-known ability to grow in colture without anchorage [8, 26]. Anchorage-independent growth is a condition where cell proliferation does not depend on colture substrate or cell-to-cell contact and has been observed for SW480 R-type and SW620 cells but not for SW480 E-type cells[8]. It has been recently demonstrated that the HCT-8 colon cancer cells become rounded and ''soft'' when, losing the mechano-sensitivity to the surrounding environment, gain this ability to grow "independently"[27]. Similarly, SW480 R-type cells could be a part of primary tumor cells which has lost sensitiveness to the environment to grow uncontrollably. On the other hand SW480 E-type cells, with a higher Stiffness, are still capable of sensing neighbouring tissues and invade them. Cells derived from lymph node metastasis (SW620 cells) have a rounded morphology similarly to SW480 R-type cells and share with them the ability to grow without anchorage. This feature is reflected in the mean cell elasticity and cytoskeleton Coherency values comparable to those obtained for SW480 R-type cells.
Conversely, cells surface appeared markedly altered in the metastatic SW620 cell line, which displayed a smoother surface



 

and a decreased Filopodia Density and Lamellipodia Area in comparison to SW480 primary tumor cells. SW620 cells are known to have a limited migration capacity compared to both populations of SW480 cells line[26]. This feature is related to the decreased number of protrusions on their surface. The smoothness of cells surface can be a consequence of the reduction of filopodia structures and/or a marker of an impairment of organization of cortical layer of cytoskeleton underlying the membrane of SW620 cells[28]. SW620 cells are representative of cancer cells that have detached from primary tumor and have invaded lymph nodes, therefore they must have acquired specific properties to survive in the lymphatic stream. Indeed, once in the vasculature, cancer cells are exposed to fluid shear forces of the stream. The majority of circulating cancer cells are rapidly and lethally damaged in the microvasculature. To survive, circulating cancer cells must adhere to the vessel walls and eventually penetrate it[29]. Cellular adhesion to a generic surface is a complex phenomenon as many simultaneous effects can affect it.

Both (i) specific and (ii) non-specific forces together contribute to the maintenance and stability of adhesion sites required for cell adhesion and spreading[14, 15].

(i) Specific forces are present as a result of receptor-ligand binding events between adhesion-associated proteins recruited to the adhesion site on the cell surface and proteins on the external environment. These recruited proteins often serve multiple purposes ranging from physical reinforcement to propagation of chemical signals and regulation of the adhesion lifetime. Important to their function, the activities of these proteins are transient; since the regulatory events governing matrix adhesions and cytoskeletal reorganization require the molecules involved to be intrinsically dynamic. Focal adhesions are molecular assemblies of clusters of multiple scaffolding and signalling proteins and their formation is based around the ligation of integrins to a specific substrate in the ECM. Contractile force imposed at adhesion sites and changes in cell shape cause the clustering of additional ligated integrins and their respective linkages to the cytoskeleton.

(ii) Non-specific adhesion forces arise from the substrate's physic-chemical characteristics and stability of adhesion sites required for cell adhesion and spreading[29]. As the for specific interactions also the role of non-specific interactions in the focal adhesions change dynamically by cytoskeletal reorganization and are equally necessary to transmit forces required for propulsion. Non-specific adhesion is mainly mediated by van der Waals attraction of the surface glycoproteins to the underlying substratum and by hydrophobic/hydrophilic interactions mediated by proteins and phospholipids. Since glycoproteins are prevalent components of the surface of most cells, non-specific adhesion is a common cellular property and in some cases non-specific adhesion can be greater than the specific[15].

Atomic force microscopy can potentially probe both interactions. Functionalized tip[30] with an ECM protein or peptide can specifically interact with some cell adhesion molecules (CAMs), whereas using hydrophobic or hydrophilic material (usually glass, silica, polyester, etc.) it is possible to measure the non-specific interactions.

We observed an increase in cell Adhesion between the cantilever and cell surface of metastatic SW620 cells which can be consequence of an altered arrangement of the cortical actin network underlying membrane, as demonstrated by Mescola and colleagues[20]. Indeed, actin network of SW620 cells, imaged with Confocal microscopy, displayed a reduction in the number of junctions compared to SW480 cells. This actin network "weakening" linearly correlates with the AFM values of non-specific Adhesion. Therefore we suggest that modification of the actin organization observed in SW620 cells is necessary to become more "sticky" to vasculature walls and be more stable in the lymphatic and blood vessels.

In several papers have been found that cancer cells are largely softer and less adhesive compared to normal/benign cells [13, 31-33]. A biomechanics comparison between metastatic MDA-MB-435 and non-metastatic MDA-MB-435/BRMS1 (435/BRMS1) human breast carcinoma cells has been recently reported [34]. Adhesion behaviour between the two cell lines were significantly different. The non-specific adhesion force was measured at 0.434 ± 0.010 nN, whereas that of 435/BRMS1 cells was 0.826 ± 0.011 nN. This adhesion force difference was ascribed to the changes in cell adhesion, cytoarchitecture, and extracellular matrix in BRMS1-expressing cells. Also metastatic cancer cells and benign mesothelial cells taken from human body cavity fluids revealed that the normal mesothelial cells was ~33% more adhesive compared to that of the metastatic cells [13]. This general behaviour, extensively reported, shows that cancer cells can strategically change their non-specific adherence and stiffness. Anyway it is mandatory to change the paradigm, indeed cancer cells don't become just less "sticky" compared to the normal cells but the non-specific adhesions can be finely modulated during all the cancer development. In this way cells that have to squeeze through tissues or other that have to adhere to vessel can modulate their membrane adhesion and cytoskeleton elasticity to better accomplish their specific tasks. Recently non-specific adhesions have been compared for malignant metastatic cells (HCT-8), malignant non-metastatic adenocarcinoma cells (Caco-2), and normal monkey kidney MA104 cells. The non-specific adhesion force for HCT-8 (metastatic) was about twice that compared to Caco-2 (non-metastatic), and insignificant for cells MA104 (normal)[16]. In this case while specific adhesion of malignant cells were reduced to facilitate their detachment from the parent tumour, the higher non-specific forces were maximized to adhere and invade the new tissues. In this context, we measured the non-specific response of cell-type-based surface adhesion by using AFM. Our analysis of the existing surface adhesive biomolecules inherent to the lymphatic metastasis compared to bulk tumour cells revealed that the cytoadhesion increases during the metastatic process. We interpret this non-specific Adhesion between the cantilever and cell surface as the result of an indispensable property acquired by metastatic cells to survive to the shear forces of the

lymphatic stream that kills the majority of circulating cancer cells [29].

## Experimental

### Cell Cultures

The SW480 and SW620 human colon carcinoma-derived cell lines were purchased from the American Type Culture Collection (ATCC; Manassas, VA) and were maintained in RPMI supplemented with 10% fetal bovine serum, penicillin-streptomycin (100 U/ml), and 2 mM L-glutamine at 37°C, in a humid 5% CO2 atmosphere, as previously reported[35]. All image analysis measurements were performed on 60 cells per sample on three independent samples.

### Scanning Electron Microscopy (SEM)

For SEM imaging, cells on coverslips were washed three times with 0.1 M Sodium Cacodylate buffer (pH 7.4) and then incubated with 0.1 M Sodium Cacodylate buffer and 2.5% glutaraldehyde for 4h. Then cells were dehydrated serially in 30%, 60%, 80% and 100% ethanol. Finally samples were fixed for 30 minutes with 2% osmium tetra-oxide ($OsO_4$). The SEM procedures were completed by drying of the samples, and sputtering of 8 nm gold layer as reported previously[36]. Micrographs were acquired with a Zeiss Supra 25 microscope (Germany) with a secondary electron detector.
In order to quantify cell morphology, cell axes were measured by means of ImageJ software. From these values, the ellipse fitting each single cell was drawn and perimeter (P) and area (A) were calculated as follows

$$P = 2\pi\sqrt{\frac{a^2+b^2}{2}}$$

$$A = \pi ab$$

where a and b are the major and minor semi axis of the cell.
The number of filopodia per cell ($N_F$) was extracted from images and normalized by the cell perimeter to obtain the density of filopodia ($\rho_F$) along the cell membrane:

$$\rho_F = \frac{N_F}{P}$$

In order to quantify the lamellipodia area, cell major ($a_B$) and minor ($b_B$) axis, were measured without taking into account the lamellipodia extensions. From these parameters, the cell ''body'' area was calculated and subtracted from the total Area (A) to recover the Lamellipodia Area ($A_L$):

$$A_L = A - \pi a_B b_B$$

It was previously reported that SW480 cell line includes two distinct subpopulations, designated as E- (epithelial) and R- (round) type[8]. Therfore, in the SW480 cell line, cells belonging to the R-type or E-type were distinguished on the basis of the Aspect Ratio (AR) defined as:

$$AR = \frac{a_B}{b_B}$$

Cells with AR higher than 1.5 were considered E-type cells.

### Atomic Force Microscopy (AFM)

Cells were kept in the cell culture medium at a constant temperature (37°C) throughout data acquisition. Cantilevers with a silica conical tip characterized by an end radius of ~10 nm and a half conical angle α of 20° have been used (CSC16-MikroMasch). We used AFM silicon probes due to its high biocompatibility and the moderate value of hydrophilicity. All these cantilevers, with a nominal spring constant of k=~0.02 N/m, were accurately calibrated by using thermal method. Force-distance (F-D) curves were obtained using a fixed force set point and keeping a constant speed of 4.0μm/s, a representative curve for each cell type are shown in Fig. 5. The total vertical displacement was set to 12 μm. F–D curves were analyzed using the data processing supplied with the JPK Nanowizard AFM system by applying baseline subtraction, conversion to tip-sample separation, identification and fitting of each jump in the retraction curve to determine the quantitative parameters described in the text. To recover the local cell Young Modulus (E) we analysed all the reaction forces F(δ) obtained from the approaching curves by using the pure elastic Hertz model for conical tips to determine an approximate starting value of E:

$$F(\delta) = \frac{2E\tan(\alpha)}{\pi(1-\nu^2)}\delta^2$$

where δ is the indentation depth and ν = 0.5 is the cells Poisson's ratio.
After an accurate Young Modulus value was obtained by using the JKR model that accounts for the adhesion for hyperboloid tip shape. Since adhesion and external load cause an elastic deformation a contact area forms between the tip and the cell, the indentation and the load respectively, can be calculated correctly as follows:

$$\delta = \frac{aA}{2R}\left[\frac{\pi}{2} + arcsin\left(\frac{(a/A)^2-1}{(a/A)^2+1}\right)\right] - \sqrt{\frac{2a\pi(1-\nu^2)\gamma_{12}}{E}}$$

and

$$F = \frac{2E}{(1-\nu^2)}\left[\frac{A}{2R}\left[aA + \frac{a^2-A^2}{2}\left(\frac{\pi}{2} + arcsin\left(\frac{(a/A)^2-1}{(a/A)^2+1}\right)\right)\right] - a\sqrt{\frac{2a\pi(1-\nu^2)\gamma_{12}}{E}}\right]$$

where R is the tip radius of curvature, A is equal to R·cot(α), $a$ is the contact radius, and $\gamma_{12}$ is the interfacial energy of the tip and the sample.

Local cell adhesion has been extracted directly from the absolute value of the force minimum in the retract curve[37, 38].

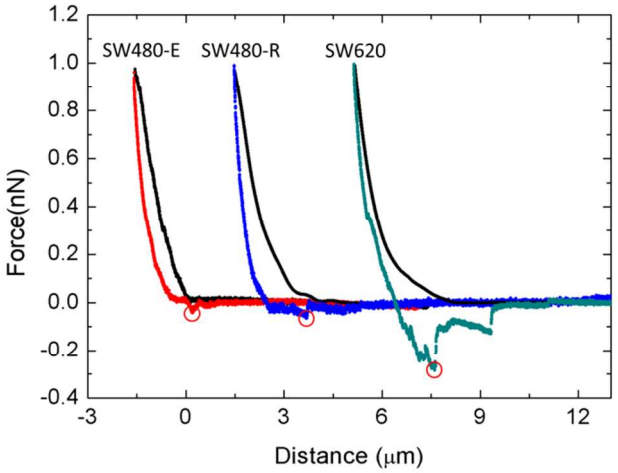


**Fig.5 Representative F-D curves obtained by AFM**. All extend curves are in black while retract curves are in red for SW480 Elongated cells, in blue for SW480 Rounded cells and in dark cyan for SW620 cells. Curves are arbitrary shifted along the x-axis for clarity. Minimum Adhesion for each curve is labelled with a red circle.

### Confocal Microscopy

For immunofluorescence cells were stained with FITC-labeled Phalloidin (Life Technologies) and DAPI (fluotomount G with DAPI, Electon Microscopy Sciences) as reported previously[39]. Immunofluorescence images were obtained with a multichannel white light source with DAPI or FITC filter settings on a CARV II spinning-disk microscope (Crisel Instruments, Rome, Italy) by using a 60X oil immersion objective (NA 1.4). Z-stacks were acquired for each sample. Background values (defined as intensities below 7% of the maximum intensity) were set to zero and coloured black as previously reported[40]. Image processing and analysis was performed with ImageJ software[41]. After having measured the Aspect Ratio of each cell in order to distinguish between elongated and rounded cells (AR threshold= 1.5), actin organization was analysed with different ImageJ plugins. Firstly, the OrientationJ plugin has been used to obtain the Coherency parameter as described previously[21]. The analysis of Coherency was performed on maximum intensity projections of the acquired Z stacks. OrientationJ evaluates the local orientation of every pixel of an image by calculating the structure tensor for each pixel. The Coherency (C) parameter is the ratio between the difference and the sum of the structure tensor eigenvalues and is bounded between 0 (isotropic areas) and 1 (highly oriented structures) [21]. To analyze the number of knots of actin network the Skeletonize tool of ImageJ has been used in order to segment 2D Z-projections. For each cell the number of junctions was calculated and normalized to cell area to obtain the Density of Junctions ($\rho_J$).

### Statistical analysis

Data were analysed by one-way ANOVA followed by Tukey's multiple comparison test. A value of $p<0.001$ was considered statistically significant.

## Conclusions

A better understanding of cells mechanics can help to predict growth and spreading ability of cancer cells. In order to investigate structural differences in cellular architecture between non-metastatic and metastatic cancer cells, we analysed the colon cancer SW480 and SW620 cell lines, which offer the unique advantage of representing different stages of disease progression of the same cancer. In fact, SW480 and SW620 cell lines were derived, respectively, from the primary tumour and a lymph-node metastasis from the same patient. Two distinct sub-populations have been described within the SW480 cell line, the E-type and R-type cells, whose name reflects their Elongated and Rounded morphology, respectively[17, 42]. Though being both derived from a primary tumour, these populations display opposite invasive properties when inoculated in nude mice: while the E-type cells have the ability to metastasize but form spontaneously regressive primary tumours, R-type cells form large primary tumors without invasion or nodal metastases[42]. On the other hand, the SW620 cell line comprises a single population of rounded metastatic cells[7].

In this article we demonstrated that cell mechanics can be related to actin organization and showed that a decrease in cell elasticity is accompanied by a high isotropy of actin fibers (SW480 R-type and SW620 cells) while a decreased number of actin network junctions is related to an increase in cell adhesion (SW620 cells) and to a smooth cell surface. We also demonstrated that mechanical stiffness and cell adhesion are modulated by cancer cells during the metastatic process.

We hypothesize that regulation of cell mechanics can allow cancer cells to acquire specialized functions essential for their ability to grow, invade surrounding tissues and metastasize. In particular soft rounded cells, insensitive to the environment, are responsible for the increase of the tumour volume thanks to their uncontrolled growth without anchorage On the other hand, elongated and highly motile cells are more prone to invade neighbouring tissues due to their high plasticity coupled to sensitiveness to the ECM. In order to cope with shear forces of the lymphatic and hematic flow, cells organize a more "flexible" cortical actin network to increase their adhesion to vessels: then, once a metastatic cell reaches a lymph node, again it modulates its mechanical properties to survive in a new environment[29].

## Acknowledgements

This research has been supported by Università Cattolica del Sacro Cuore of Rome. Measurements were performed at the Laboratorio Centralizzato di Microscopia ottica ed elettronica facility (LABCEMI) of Università Cattolica del S. Cuore (Rome, Italy). We are extremely thankful to Mario Amici for the technical support in experiments.

## Notes and references

[a] Institute of Physics, Università Cattolica del Sacro Cuore, Rome, Italy.
[b] Institute of Pathology, Università Cattolica del Sacro Cuore, Rome, Italy.
*Equally contributed
& Share the seniorship of this article

Electronic Supplementary Information (ESI) available: [details of any supplementary information available should be included here]. See DOI: 10.1039/b000000x/

1 P. Katira, R.T. Bonnecaze, M.H. Zaman, *Front. Oncol.*, 2013, **3**:145 doi: 10.3389/fonc.2013.00145
2 E. L. Baker, R. T. Bonnecaze, M. H. Zaman, *Biophys. J.*, 2009, **97**, pp. 1013–1021
3 M. Guo, A. J. Ehrlicher, M. H. Jensen, M. Renz, J.R. Moore, R.D. Goldma, J. Lippincott-Schwartz, F.C. Mackintosh, D.A. Weitz, *Cell*, 2014, **158**, pp. 822-832
4 J.I. Lopez, J.K. Mouw, V.M., *Oncogene*, 2008, **27**, pp. 6981-6993.
5 S. Suresh, *Acta Biomater.*, 2007, **3** pp. 413–438.
6 G. Halder, S. Dupont, S. Piccolo, *Nat. Rev. Mol. Cell Biol.*, 2012, **13**, pp. 591-600.
7 R.E. Hewitt, A. McMarlin, D. Kleiner, R. Wersto, P. Martin, M. Tsokos, G.W. Stamp, W.G. Stetler-Stevenson, *J. Pathol*, 2000, **192**, pp. 446-454.
8 N. Tomita, W. Jiang, H. Hibshoosh, D. Warburton, S.M. Kahn, I.B. Weinstein, *Cancer Res.*, 1992, **52**, 24 6840-6847.
9 G.J. Liefers, A.M. Cleton-Jansen, C.J. van de Velde, J. Hermans, J.H. van Krieken, C. J. Cornelisse, R.A. Tollenaar, *N. Engl. J. Med.* 1998 **339** pp.223-228.
10 A. Leibovitz, J.C. Stinson, W.B. McCombs, C.E. McCoy, K.C. Mazur, N.D. Mabry, *Cancer Res.* 1976; **36** pp. 4562–4569
11 E.J. Luna, A.L. Hitt, *Science* 1992 **258** pp. 955-964
12 M. Plodinec, M. Loparic, C.A. Monnier, E.C. Obermann, R. Zanetti-Dallenbach, P. Oertle, J.T. Hyotyla, U. Aebi, M. Bentires-Alj, R.Y. Lim, C.A. Schoenenberger, *Nat Nanotechnol.* 2012, **7** pp.757-765.
13 S.E. Cross, Y.S. Jin, J. Rao, J.K. Gimzewski, *Nat Nanotechnol.*, 2007, **22**, pp. 780-783.
14 M.H. Lee, D.A. Brass, R. Morris, R.J. Composto, P. Ducheyne *Biomaterials*, 2005, **26**, pp. 1721–1730.
15 W.F. Loomis, D. Fuller, E. Gutierrez, A. Groisman, W.J. Rappel, *PLoS ONE*, 2012 **7** pp, e42033
16 X. Tang, T. Cappa, T. Kuhlenschmidt, M. Kuhlenschmidt, T. Saif. in *Mechanobiology of Cell-Cell and Cell-Matrix Interactions*. ed. Wagoner Johnson, A., Harley, Brendan (Eds.) 2011, pp 105-122
17 V. Palmieri, D. Lucchetti, A. Maiorana, M. Papi, G. Maulucci, G. Ciasca, M. Svelto, A. Sgambato, M. De Spirito, *Appl. Phys. Lett.*, 2014, **105** (12) Art. No. 123701
18 H. Butt, B. Cappella, M. Kappl, *Surf. Sci. Rep.*, 2005, **59** pp. 1–152
19 M. Sun, J.S. Graham, B. Hegedüs, F. Marga, Y. Zhang, G. Forgacs, M. Grandbois. *Biophys. J.* 2005, **89** pp. 4320–4329.
20 A. Mescola, S. Vella, M. Scotto, P. Gavazzo, C. Canale, A. Diaspro, A. Pagano, M. Vassalli, *J. Mol. Recognit.*, 2012, **25**, pp. 270-277.
21 R. Rezakhaniha, A. Agianniotis, J.T. Schrauwen, A. Griffa, D. Sage, C.V. Bouten, F.N. van de Vosse, M. Unser, N. Stergiopulos, *Biomech. Model. Mechanobiol.*, 2012, **11**, pp. 461-473.
22 M. Yilmaz, G. Christofori, *Mol. Cancer Res.*, 2010, **8**, 5 629-642.
23 S.H. Doak, D. Rogers, B. Jones, L. Francis, R.S. Conlan, C. Wright, Histochem. Cell Biol., 2008, 909-916.
24 H. Yamaguchi, J. Condeelis, *Biochim. Biophys. Acta.*, 2007, **1773**, pp. 642-652.
25 R.P. Stevenson, D. Veltman, L.M. Machesky, *J. Cell Sci.*, 2012, **125** pp.1073-1079
26 B.S. Kubens, K.S. Zänker, *Cancer Lett.,* 1998, **131**, 55-64.
27 X. Tang, Q. Wen, T.B. Kuhlenschmidt, M.S. Kuhlenschmidt, P.A. Janmey, T.A. Saif, *Plos One*, 2012, **7** pp. e50443
28 M.E. Dokukin, N.V. Guz, R.M. Gaikwad, C.D. Woodworth, I. Sokolov, *Phys. Rev. Lett.*, 2011, **107**, pp. 028101.
29 T. Korb, K. Schlüter, A. Enns, H.U. Spiegel, N. Senninger, G.L. Nicolson, J. Haier, *Exp. Cell Res.*, 2004, **299**, pp. 236-247.
30 G. Lama, M. Papi, C. Angelucci, G. Maulucci, G. Sica, M. De Spirito, *PLoS One*. 2013, **8** pp. e52530.
31 S.E. Cross, Y.S. Jin, J. Tondre, R. Wong, J. Rao, J.K. Gimzewski *Nanotechnology*, 2008, **19** pp. 384003–384011
32 M. Lekka, P. Laidler, D. Gil, J. Lekki, Z. Stachura, A.Z. Hrynkiewicz *Eur. Biophys. J.*, 1999, **28** pp. 312–316
33 N. Bao, Y.H. Zhan, C. Lu Anal. Chem., 2008, **80** pp. 7714–7719
34 Y. Wu, G.D. McEwen, S. Harihar, S.M. Baker, D.B. DeWald, A. Zhou, *Cancer Lett.*, Vo, 2010, **293**, pp. 82-91
35 A. Sgambato, M.A. Puglisi, F. Errico, F. Rafanelli, A. Boninsegna, A. Rettino, G. Genovese, C. Coco, A. Gasbarrini, A. Cittadini, *J. Cell. Physiol.*, 2010, **224** pp. 243-241.
36 G. Ciasca, L. Businaro, M. Papi, A. Notargiacomo, M. Chiarpotto, A. De Ninno, V. Palmieri, S. Carta, E. Giovine, A. Gerardino, M. De Spirito, *Nanotechnology*, 2013, **24**, pp. 495302.
37 M. Papi, P. Paoletti, B. Geraghty, R. Akhtar, *Appl. Phys. Lett.*, 2014, **104** Art. No. 103703
38 F. Bugli, B. Posteraro, M. Papi, R. Torelli, A. Maiorana, F. Paroni Sterbini, P. Posteraro, M. Sanguinetti, M. De Spirito, *Antimicrob Agents Chemother.*, 2013, **57** pp. 1275-1282.



 

39 N. Di Simone, M. De Spirito, F. Di Nicuolo, C. Tersigni, R. Castellani, M. Silano, G. Maulucci, M. Papi, R. Marana, G. Scambia, A. Gasbarrini, *Biol. Reprod.*, 2013, **89** pp. 88.

40 G. Maulucci, D. Troiani, S.L. Eramo, F. Paciello, M.V. Podda, G. Paludetti, M. Papi, A. Maiorana, V. Palmieri, M. De Spirito, A.R. Fetoni, *Biochim. Biophys. Acta.*, 2014, **1840** pp. 2192-2202.

41 J. Schindelin, I. Arganda-Carreras, E. Frise, V. Kaynig, M. Longair, T. Pietzsch, S. Preibisch, C. Rueden, S. Saalfeld, B. Schmid, J.Y. Tinevez, D. J. White, V. Hartenstein, K. Eliceiri, P. Tomancak and A. Cardona, *Nat. Methods*, 2012, **9**, pp. 676-682

42 W.H. Yoon, S.K. Lee, K.S. Song, J.S. Kim, T.D. Kim, G. Li, E.J. Yun, J.Y. Heo, Y.J. Jung, J.I. Park, G.R. Kweon, S.H. Koo, H.D. Park, B.D. Hwang, K. Lim, *Mol. Med Rep.*, 2008, **1**, pp. 763-768.

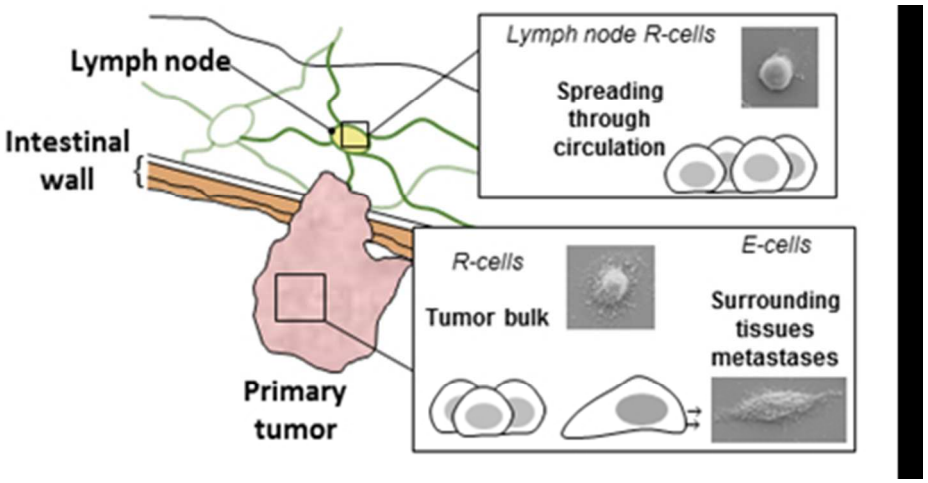


Sketch of intestinal wall invasion occurring during colon cancer development. Regulation of cell morphology and mechanics allows cancer cells to acquire specialized functions. In primary tumor soft rounded cells, insensitive to the environment, are responsible for the increase of the cancer volume, while elongated and highly motile cells invade neighbouring tissues.
In the lymph node, in order to cope with shear forces of the lymphatic, rounded cells organize a more "flexible" cortical actin network to increase their adhesion to vessels
81x39mm (150 x 150 DPI)